PAPER

Effective monitoring of landfills: flux measurements and thermography enhance efficiency and reduce environmental impact

IOP Publishing Journal of Geophysics and Engineering
J. Geophys. Eng. **10** (2013) 064002 (14pp) doi:10.1088/1742-2132/10/6/064002

Effective monitoring of landfills: flux measurements and thermography enhance efficiency and reduce environmental impact

Raffaele Battaglini[1], **Brunella Raco**[2] **and Andrea Scozzari**[3]

[1] Chemgeo sas, Follonica (GR), Italy
[2] Consiglio Nazionale delle Ricerche (CNR-IGG), Pisa, Italy
[3] Consiglio Nazionale delle Ricerche (CNR-ISTI) Italy, Pisa, Italy

E-mail: chemgeo@gmail.com, b.raco@igg.cnr.it and a.scozzari@isti.cnr.it

Received 29 March 2013
Accepted for publication 18 September 2013
Published 25 November 2013
Online at stacks.iop.org/JGE/10/064002

Abstract
This work presents a methodology for estimating the behaviour of a landfill system in terms of biogas release to the atmosphere. Despite the various positions towards the impact of methane on global warming, there is a general agreement about the fact that methane from landfill represents about 23% of the total anthropogenic CH_4 released to the atmosphere. Despite the importance of this topic, no internationally accepted protocol exists to quantify the leakage of biogas from the landfill cover. To achieve this goal, this paper presents a field method based on accumulation chamber flux measurements. In addition, the results obtained from a nine-year-long monitoring activity on an Italian municipal solid waste (MSW) landfill are presented. The connection between such flux measurements of biogas release and thermal anomalies detected by infrared radiometry is also discussed. The main overall benefit of the presented approach is a significant increase in the recovered energy from the landfill site by means of an optimal collection of biogas, which implies a reduction of the total anthropogenic methane originated from the disposal of waste.

Keywords: landfill, biogas, environmental impact, geostatistics, thermography

(Some figures may appear in colour only in the online journal)

Introduction

In the majority of industrialized and developing countries, landfill is the destination for most municipal and industrial waste, as it is still the most utilized methodology for waste management. Many authors define landfills as bioreactors where waste undergoes aerobic degradation processes, until the oxygen is totally consumed. Therefore, waste is decomposed by non-methanogenic bacteria (i.e., organisms that do not produce methane as a direct metabolic product), which convert organic compounds into organic acids with a simple structure. These simple substances are further transformed into CO_2 and CH_4 by those bacteria that are present mainly in the leachate (Wolfe 1971, Zeikus 1977, Balch *et al* 1979, Boone and Bryant 1980, McInerey and Bryant 1980, 1981a, 1981b, Mah and Smith 1981, Anthony 1982, Kirshop 1984, Whitman 1985). These gases, called biogas or landfill gas (LFG), are a mixture of methane (40–45 vol.% on average) and carbon dioxide (55–60 vol.% on average), nitrogen and other trace species, often toxic and malodorous. It is commonly considered that methane from landfill represents about 23% of the total anthropogenic CH_4 discharged into the atmosphere (US-EPA, 2009), thus contributing significantly to global warming. Following the IPCC (2006), the global

warming potential (GWP) of methane is 23 times stronger than that of CO_2. For instance, the GWP of methane is 63 times stronger than that of CO_2 for a time horizon of 20 years, whereas the ratio between the GWP of CH_4 and that of CO_2 reduces to 20 for a time horizon of 100 yr (Simpson and Anastasi 1993). In spite of these different opinions on the GWP of CH_4, there is a general consensus on the role of the gas generated by the landfill and discharged through their cover into the atmosphere, which is unanimously considered to represent one of the most important contributions to the global greenhouse effect.

A significant fraction (more than 60%) of the LFG produced escapes from the landfill cover, even when collecting systems are properly installed. Many numerical models, able to foresee LFG production from waste, have been developed (Findikakis and Leckie 1979, El-Fadel *et al* 1988, Findikakis *et al* 1987, Manna *et al* 1999, Nastev *et al* 2001, Hashemi *et al* 2002, Scharff 2006). These models are based on theoretical data about waste amount and typology, the kinetics of organic matter degradation and the methane generation rate, and are often, unfortunately, the only way used to size the LFG recovery plant and to check the efficiency of the system. The interest in predicting the amount of biogas produced which is released to the atmosphere, spread also to the experimentation of data-driven modelling approaches, applied to time series of biogas fluxes directly measured at the cover–atmosphere interface (Scozzari 2008, Li *et al* 2011).

This kind of merely theoretical approach precludes the complete understanding of the inefficiencies of the energy recovery system and its causes. In particular, numerical models do not allow an understanding whether low efficiency is due to a production lower than the expected one or to a dispersion higher than the estimated one. This problem can be solved by an empirical tool based on real field measurements of CO_2 and CH_4 fluxes from the soil that covers the landfill, with the result of optimizing the overall efficiency of the plant. In other words, for the proper management of a landfill site in terms of economic costs and environmental issues, it is necessary to set up an affordable method in order to check the real impact of restraining and collecting systems. Despite the importance of this topic, no internationally accepted protocol exists to quantify the LFG leakage from the landfill cover.

This work presents a field method based on direct flux measurements from the landfill surface, made by an accumulation chamber method. Furthermore, the results obtained from a nine-year-long monitoring activity on a municipal solid waste (MSW) landfill located in Italy are presented. The connection between such flux measurements of biogas release and thermal anomalies detected by infrared radiometry is also discussed.

From May 2004 to December 2012, nineteen soil gas emission surveys and 18 thermographic surveys were carried out at the MSW landfill of Legoli (Peccioli municipality, Pisa province, Italy). The investigated landfill (figure 1) is located in the Val d'Era Graben, Central Tuscany (Mazzanti 1961, Martini and Sagri 1993). A clay formation with a permeability of about 10^{-9} cm s^{-1} constitutes the impervious substrate. The area of the landfill surface is approximately 140 000 m^2.

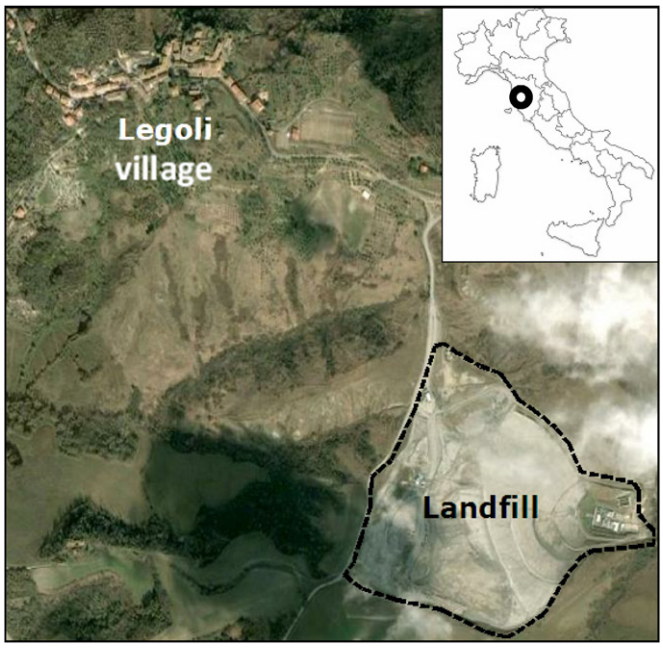

Figure 1. Location of the Legoli landfill (Peccioli, Pisa, Italy).

Until 2007, when the landfill was closed, a total of 3,100 000 t of MSW were disposed of in the Legoli plant, with a daily amount of managed wastes of 700–1000 t d^{-1}. The landfill has a collecting system, which consists of about 120 wells and a power plant that generated approximately 5000 MWh in 2002 and 2003 and 7500 MWh in 2006 and 2007.

Mapping biogas fluxes

LFG fluxes from the landfill cover have been mapped by means of data processing performed by the ISATIS program, employing the kriging method to extrapolate values where the measures are missing (Krige 1951, Matheron 1962, 1965, 1969, 1970, Clark 1979, David 1977, Davis 1986). This method starts from the construction of an experimental variogram, and has the peculiarity to assure that interpolated values have an unbiased mean value and minimum variance (Chauvet 1982, 1991, 1993, Chauvet and Galli 1982, Armstrong 1984a, 1984b, Wackernagel 1995).

Nevertheless, the global estimation of LFG cannot be done by utilizing the kriging technique. In fact, the global mean is very unlikely to be directly kriged (Journel and Huijbregts 1978), since it is not usually possible to assume stationarity over the entire area, but only over limited neighbourhoods (i.e., local quasi-stationarity). Moreover, the construction of such a kriging matrix would imply that the structural functions, covariance $C(h)$ or semivariance $\gamma(h)$, are known up to a distance h, having the order of dimensions of the area, and the limit of reliability of an experimental semi-variogram is a distance $L/2$, half of the field dimensions.

For these reasons, the total diffuse gas output has been estimated by following the statistical approach described by Sinclair (1974, 1991), which consists of (i) the partitioning of the flux data by means of cumulative probability plots; (ii) the computation of the arithmetic mean of raw data (AMRD)

for each partitioned population, and (iii) the calculation of the 95% confidence interval of the mean using the Sichel's *t*-estimator (Sichel 1966, David 1977). Before every kind of statistical data processing, the presence of outliers has been tested by means of both box–whisker plots and an analytical process based on the central limit theorem (Singh 1993, Sigh *et al* 1997).

According to the procedure described in this paper, outliers have been eliminated from the original data set as a preliminary action. Values lower than the instrumental detection limits (0.02 mol m^{-2} d^{-1} for CO_2 and 0.05 mol m^{-2} d^{-1} for CH_4) have also been omitted. This choice causes a substantial increase of the mean CO_2 and CH_4 fluxes. However, the portion of the surface area corresponding to these undetectable values has been neglected, in order to avoid any influence on the total LFG output.

Nevertheless, the estimation of the LFG output released into the atmosphere does not allow the direct determination of the efficiency of the collecting system, which can be evaluated by:

$$\eta = \mathrm{LFGcapt}/(\mathrm{LFGcapt} + \mathrm{POG}), \quad (1)$$

where LFGcapt is the amount of LFG captured by the collecting system and POG is the pre-oxidation gas. POG represents the actual amount of LFG lost by the collecting system, which is higher than the total LFG release estimated by the flux measurement at the landfill cover–air interface, due to the effects induced by CH_4 oxidation processes occurring in the shallower layer of the landfill cover (Czepiel *et al* 1996, Le Mer and Roger 2001, Chanton and Liptay 2000, Barlaz *et al* 1989). For this reason, in order to evaluate the amount of POG it is necessary to correct the estimation of LFG flux, taking into account the overall reaction describing the oxidation processes occurring in the subsurface zone (De Visscher and Van Cleemput 2003):

$$CH_4 + 1.5\ O_2 \rightarrow 0.5\ CO_2 + 1.5\ H_2O_{(liq)} + 0.5\ CH_2O, \quad (2)$$

where CH_2O represents the average composition of the formed biomass. Based on the stoichiometry of reaction (2) and knowing the CH_4/CO_2 molar ratio in the POG, it is possible to compute the production of CO_2 and CH_4 ($\varphi_{CO2,d}$ and $\varphi_{CH4,d}$), before the subsurface oxidation processes occur:

$$\varphi_{CO_2,d} = \varphi_{CO_2,m} - 0.5\Delta \quad (3)$$

$$\varphi_{CH_4,d} = \varphi_{CH_4,m} + \Delta, \quad (4)$$

where $\varphi_{CO2,m}$ and $\varphi_{CH4,m}$ are the measured fluxes of CO_2 and CH_4, and Δ represents the amount of methane consumed by reaction (2). Alternatively, if methane oxidation is assumed to occur without biomass production, according to the reaction (De Visscher and Van Cleemput 2003):

$$CH_4 + 2O_2 \rightarrow CO_2 + 2\ H_2O_{(liq)}, \quad (5)$$

the POG entity can be computed by means of the following equations:

$$\varphi_{CO_2,d} = \varphi_{CO_2,m} - \Delta \quad (6)$$

$$\varphi_{CH_4,d} = \varphi_{CH_4,m} + \Delta. \quad (7)$$

Average fluxes of deep CO_2 and deep CH_4 have been summed to obtain the flux of POG. Knowing POG, it is possible to calculate the efficiency of the collecting system, by means of equation (1).

Moreover, the POG flux plus the amount of LFGcapt can be used to estimate the total LFG produced, and this last estimation can be compared with the output of numerical production models. Since landfill sites change from survey to survey, this comparison has been carried out referring to specific fluxes, i.e., fluxes per unitary surface area.

Infrared radiation thermometry

A thermographic device produces a map of the surface temperature in the observed scene, derived by a measurement of the distribution of radiation intensities in particular spectral bands. Thus, the radiometric measurement is not directly presented to the user, but the instrument performs a signal processing procedure that includes an inversion of Planck's law, under the assumption that targets are characterized by a spectrally constant emissivity (i.e., a grey body or black body approximation). A good reference to go deeper into aspects relating to radiation thermometry can be found in Dewitt and Nutter (1988).

Depending on the objectives of the observational survey and the kind of targets observed, the interest may be restricted to a mere vision in the infrared band, rather than the execution of real radiometry. In the first case, the apparatus will have no special requirements for the measurement of the radiation received, in terms of stability and precision, and it is typically defined as an 'imager'. In the second case, a real measuring instrument is needed, which provides a quantitative determination of the incoming radiation, and applies the radiometric equations for the extraction of temperature information about the objects inside the observed scene. What is usually obtained from an instrument of this type is a real-time map of temperatures shown in false colour or greyscale. The accuracy required from a radiometric instrument involves particular technical details and signal processing strategies, which are required in order to obtain a map of temperature corrected with respect to the various known interfering effects (e.g., the background radiation, environmental temperature, atmospheric effects and target emissivity). It is not commonly feasible to get the information necessary in order to make measurements of absolute temperature values, especially in environmental applications. In particular, the variability of environmental conditions (e.g., the atmospheric temperature and diurnal irradiation) and of the observed targets (e.g., modifications in the soil coverage and vegetation) make it necessary to think in comparative terms (i.e., by looking at differences between targets with known radiometric properties and targets under study). It is thus clear that relative (but still quantitative) measurements need an in-depth interpretation capability which takes into account the radiometric peculiarities of the particular working context, and that requires a specific expertise by the user.

Given Planck's formula for the spectral radiance of a black body:

$$L_{bb}(\lambda, T) = \frac{2 \cdot h \cdot c^2}{\lambda^5} \cdot \frac{1}{(e^{\frac{h \cdot c}{\lambda \cdot K \cdot T}} - 1)}, \quad (8)$$

where h is the Planck constant, K the Boltzmann constant, c the speed of the light, and L_{bb} is the radiance emitted at wavelength λ by a black body kept at temperature T; the temperature of an eventual black body from which a given amount of radiance is received, can be obtained by the inversion of equation (8).

The sensor actually integrates the incoming radiance on a finite wavelength interval. It is thus reasonable to express the incoming radiation in terms of spectral radiance, which is defined as:

$$L_\lambda = \frac{\partial L}{\partial \lambda} = \frac{\partial^3 \Phi}{\partial \Omega \partial s \partial \lambda} (\mathrm{W\ m^{-2}\ sr^{-1}\ \mu m^{-1}}), \tag{9}$$

where ϕ is the radiation flux per elementary solid angle $\partial\Omega$ and surface ∂s, for an elementary wavelength interval.

The temperature maps displayed by a thermographic device can be calculated under the hypothesis of a spectrally constant non-unitary emissivity of the observed target (i.e., a grey body hypothesis). If an hypothesis of unitary emissivity is applied (i.e., an opaque body that emits or absorbs radiation with no transmission) the temperature maps show an equivalent black body temperature of the observed targets, i.e., the temperature that a black body would have in order to emit that amount of radiation.

The known Wien relation:

$$\lambda_{\max} = \frac{b}{T}, \tag{10}$$

where $b = 2897.8\ \mu$m K is the Wien constant and T is a temperature expressed in Kelvin, shows that an hypothetical target at 300 K emits the maximum radiation at a wavelength close to 10 μm. This justifies the usage of infrared radiometers operating in the long-wave infrared (or thermal infrared) spectral region for environmental applications.

Extended information about infrared thermography can be found in the book by Gaussorgues (1993), listed in the references.

Instrumentation and method

Gas flux measurements

The accumulation chamber method has been utilized to measure CO_2 fluxes from the soil since the 1970s. This method is based on the determination of the rate of increase of the CO_2 concentration inside a chamber placed on the soil surface. This static technique has been successfully used in the agricultural sciences in order to determine soil respiration (Witkamp 1969, Kucera and Kirkham 1971, Kanemasu *et al* 1974, Parkinson 1981), to measure the flux from the soil of other gaseous species, e.g., N_2O (Kising and Socolow 1994) and to evaluate the total diffuse CO_2 output in volcanic and geothermal areas (Tonani and Miele 1991, Chiodini *et al* 1996, 1998).

This method is preferable to other techniques such as those based on dynamic concentrations, *in situ* gas concentration measurements at different depths, tracer gases and eddy correlation. Furthermore, Trégourès *et al* (1999) demonstrated that the accumulation chamber method is less dependent on meteorological conditions compared to other methodologies. However, the influence of meteorological conditions such as rain and soil humidity can be avoided by working in a dry season. The influence of barometric pressure on soil gas concentration and fluxes is generally high (Reimer 1980, Hinkle and Ryder 1987, 1988, Hinkle 1994, King and Minissale 1994, Pinoult and Baubron 1996), so, in order to evaluate the influence of P_{atm}, repeated measurements can be carried out at some sites located in the landfill area, thus and characterizing the flux–pressure relationship.

The used instrument (a flux Meter by West Systems Srl) consists of (figure 2):

- a circular accumulation chamber, 10 cm high with a surface of 314 $\mathrm{cm^2}$;
- two IR spectrophotometers, which measure CO_2 and CH_4 concentrations;
- an analogue-to-digital converter;
- a palm-top computer;
- a Global Positioning System (GPS).

For CO_2 determination a LI-COR LI 820 IR detector, with a range of 0–20 000 ppmv and an analytical accuracy of 2%, has been used, while a purpose-made IR detector (West Systems WSHC), with a range of 0–50 000 ppmv and an accuracy of 5%, has been used for the measurement of CH_4 (Virgili *et al* 2008). A dedicated application displays directly on the field the concentration of measured gases (CO_2 and CH_4) versus the measurement time. The initial slope of this curve is proportional to the gas flux from the soil (φ_{soil}). The reliability of this instrument has been proved (Raco *et al* 2010 and references therein), as well as its ability to provide fast measurements (about 1 min for each measurement point).

Laboratory tests were performed before each survey in order to calibrate the measurement system. The obtained reproducibility is better than 1% for high fluxes (>10 mol $\mathrm{m^{-2}\ d^{-1}}$) and about 5% for low fluxes (<1 mol $\mathrm{m^{-2}\ d^{-1}}$).

Infrared thermography

Thermographic images have been taken with a long-wave IR radiometer in the same period of each biogas survey, for cross-validation purposes. One interesting aspect of such an approach is the possibility of identifying the degree of correlation between eventual thermal anomalies and the local biogas release into the atmosphere.

The apparatus used for the execution of these campaigns were all based on FPA (focal plane array) type sensors, i.e., sensors that do not require the mechanical scanning of the image, having a number of detectors arranged in array equal to or higher than the number of image pixels.

The matrices FPA can be divided into two classes: (i) photon counters; and (ii) heat detectors. Photon counters convert photons associated with the incident infrared radiation in electrons, which are then detected and counted. Such devices need to operate at cryogenic temperatures, typically around 77 K, implying the use of a heat pump based on some mechanical hardware (e.g., a Stirling cycle machine). Heat detectors perform an indirect radiometric measurement by converting the energy associated with the collected radiation into heat, which is measured by each individual sensor element. In the case of microbolometer sensors, the variation of the local

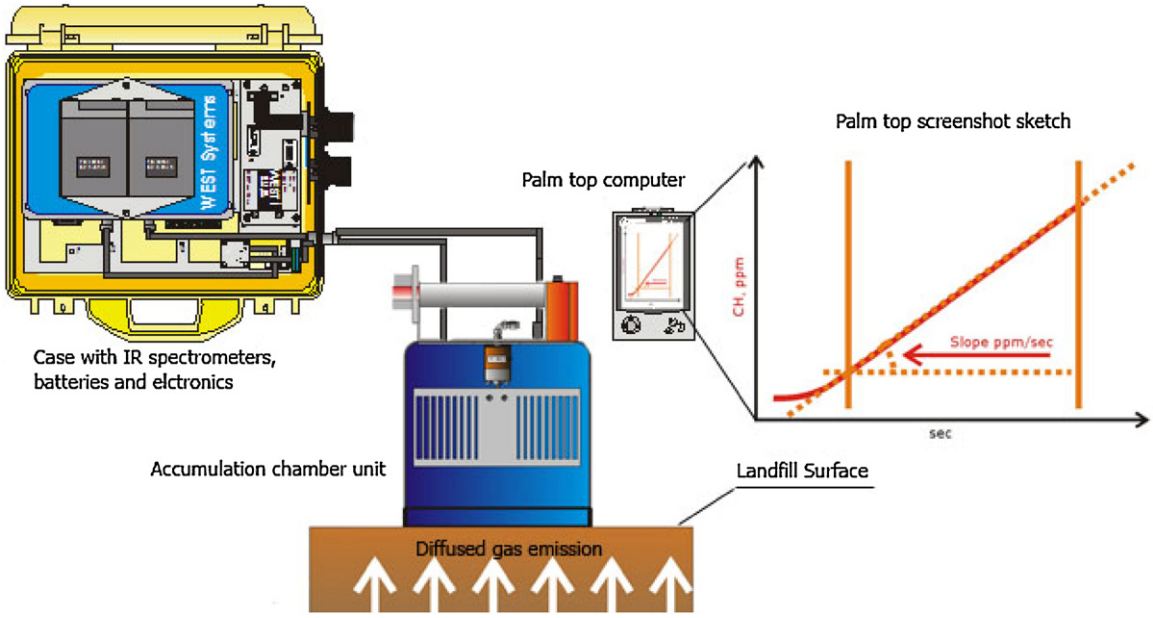

Figure 2. Sketch of the adopted instrumentation.

temperature of each single detector in the array is converted into electrical information by an elementary device sensitive to temperature (usually a thermistor).

A claimed feature of this family of sensors is the ability to operate at (almost) room temperature; in fact, even though they are extremely sensitive to changes in their operating temperature and require an excellent thermal stabilization of the array, proper operation is obtained at temperatures around 250 K, which are usually obtained with solid-state Peltier elements.

This class of thermal imaging cameras is particularly interesting for all those applications which require continuous monitoring. On the other hand, the sensitivity to small temperature changes in the array of detectors makes these devices somewhat prone to produce artefacts, with stability and accuracy figures generally lower than those currently obtainable from arrays of cooled detectors.

Finally, a considerable advantage of microbolometer detectors resides in the spectral region in which they operate; in fact, the far infrared region is characterized by a drastic reduction in the effect of the reflected solar radiation (compared to mid-infrared sensors); this can be easily understood by looking at equation (10), which shows how the usage of longer wavelengths in the infrared region go further from the emission peak of solar radiation (supposing the sun surface to be a black body set at 6000 K, thus peaking almost in the middle of the visible band).

During the period covered by this investigation, thermal images have been taken by infrared radiometers based on the microbolometer technique. Three different devices have been used during the period covered in this paper: an Inframetrics model PM295, manufactured by FLIR/Inframetrics (USA); a FLIR B360, from the same manufacturer; and a TH7102, manufactured by NEC (Japan). All these instruments share several common features; in fact, they all have a resolution of 320 $\times$ 240 pixels and operate in the long-wave infrared band (with a slightly wider band for the B360 and an even larger one for the TH7102), and a field of view of about 25° $\times$ 19°, incremented to 29° $\times$ 22° for the NEC.

In this particular field of application, thermography appears to have a double advantage: (i) it facilitates the validation of the distribution of the gaseous emissions; and (ii) it enhances the possibility of understanding the observed processes by individuating the degree of correlation between relative thermal anomalies (with respect to the average apparent temperatures) and biogas flux (Raco *et al* 2005). In fact, surficial thermal anomalies would rather represent a tendency to produce biogas, but the eventual emission towards the atmosphere is not a necessary consequence, because it depends on the quality of the coverage and of the gas collecting systems. This means that high gas fluxes may be measured in the presence of low surficial temperatures because of inappropriate collecting systems, plus relevant thermal anomalies may be associated with poor gas flux, thanks to an efficient coverage and collection system.

The case study

Nineteen flux surveys and 18 thermographic surveys were carried out on Legoli landfill over nine years from 2004 to 2012. In October 2004, the same kind of survey was carried out with the collecting system at rest, to understand its influence on the total LFG output.

Biogas flux

The main statistical parameters of the raw data collected by the flux campaigns are reported in table 1.

The measured fluxes vary from undetectable values (see above) to 1040 mol m^{-2} d^{-1} for CH_4 and 890 mol m^{-2} d^{-1} for CO_2.

For each of the 19 surveys, geostatistical data processing has been carried out and an experimental semivariogram

Table 1. Main statistical parameters of the raw data. Data are expressed in mol m^2 d^{-1}.

Survey	Gas	Points	Mean	Median	Min	Max	St. dev.	Skewness
May 2004	CO_2	110	3.45	1.31	0.00	63.12	7.62	5.53
	CH_4	110	2.99	0.00	0.00	84.10	9.95	6.04
October 2004	CO_2	267	18.67	2.90	0.00	259.45	45.91	3.75
	CH_4	265	15.42	1.91	0.00	217.07	40.02	3.62
January 2005	CO_2	161	3.49	1.43	0.00	33.74	5.66	2.54
	CH_4	161	3.40	1.33	0.00	35.58	6.09	2.99
May 2005	CO_2	318	7.91	0.93	0.00	274.97	25.75	6.41
	CH_4	318	4.39	0.48	0.00	201.68	16.62	7.25
October 2005	CO_2	305	6.58	1.02	0.00	235.55	19.21	7.61
	CH_4	306	3.56	0.25	0.00	189.03	16.52	8.24
May 2006	CO_2	282	9.19	1.58	0.00	237.45	24.59	5.32
	CH_4	282	4.86	0.44	0.00	161.90	15.53	6.10
October 2006	CO_2	300	11.09	2.79	0.00	257.47	26.99	5.47
	CH_4	302	6.88	0.56	0.00	245.53	22.34	6.33
June 2007	CO_2	294	4.51	1.42	0.00	212.33	14.15	11.47
	CH_4	295	2.97	0.35	0.00	154.75	12.32	9.55
November 2007	CO_2	301	4.40	0.66	0.00	185.90	13.73	8.75
	CH_4	301	2.90	0.00	0.00	141.90	10.89	8.56
July 2008	CO_2	353	3.39	1.28	0.00	46.44	5.71	4.29
	CH_4	353	2.40	0.32	0.00	66.87	6.69	6.12
January 2009	CO_2	332	4.15	0.33	0.00	517.50	29.41	16.28
	CH_4	332	2.21	0.10	0.00	109.60	9.51	7.75
June 2009	CO_2	307	3.87	1.09	0.00	81.52	8.36	4.80
	CH_4	311	3.82	0.29	0.00	107.49	12.27	5.37
December 2009	CO_2	299	2.45	0.55	0.00	125.19	8.21	11.80
	CH_4	299	1.89	0.15	0.00	106.87	7.31	10.82
June 2010	CO_2	281	2.67	0.99	0.00	101.50	8.54	9.88
	CH_4	281	1.71	0.13	0.00	129.96	9.99	10.94
December 2010	CO_2	212	1.45	0.33	0.00	55.70	5.19	8.01
	CH_4	212	1.09	0.00	0.00	65.39	5.95	8.76
May 2011	CO_2	362	1.08	0.38	0.00	29.29	2.51	6.75
	CH_4	362	0.41	0.09	0.00	13.26	1.44	6.54
November 2011	CO_2	269	2.00	0.30	0.00	78.90	6.83	7.38
	CH_4	269	1.60	0.10	0.00	97.90	7.90	9.20
May 2012	CO_2	301	1.34	0.52	0.00	43.59	3.41	8.55
	CH_4	301	0.67	0.14	0.00	43.28	3.35	10.68
November 2012	CO_2	226	6.51	0.27	0.00	889.81	62.77	13.04
	CH_4	226	7.54	0.20	0.00	1041.50	74.59	12.69

has been built. Generally, the observed spatial variability for both CO_2 and CH_4 fluxes as well as of the total LFG flux can be represented by a spherical model with a nugget effect. Table 2 suggests that the spatial variability of fluxes can be described by a semivariogram with a mean range of influence of about 100 m and a Sill (variance) of 2 (mol m^2 $d^{-1})^2$, with a contribution due to a nugget effect of around 1 (mol m^2 $d^{-1})^2$. It is interesting to note that the last four surveys show a decrease of the range value. This effect is probably linked to the decrease of total diffuse emission, as shown in table 3, presumably due to landfill aging and/or to an improved efficiency of the impervious cover.

Isoflux maps have been drawn by geostatistical data processing (lognormal kriging). The reliability of the interpolating models has been verified through the cross-validation technique (Clark 1979). Examples of the experimental semivariogram, interpolating model, cross-validation diagrams and resulting isoflux map, as well the standard deviation map, are shown in figure 3. The data shown relate to the June 2010 survey.

To reconcile data representativeness with the time needed to map the entire landfill, flux measurements were carried out over a regular grid of about 20 m $\times$ 20 m covering the entire landfill surface, apart from the active disposal area. The GPS, integrated with the purpose-made software running on the palmtop computer, ensured the correct positioning of every single measurement with an uncertainty of 2–3 m.

The influence of meteorological conditions was reduced by working in steady dry weather days and completing each flux survey in two working days.

In order to evaluate the total LFG output, data were processed following the partitioning method described by Sinclair (1974, 1991) and frequently used in the pertinent geochemical literature (e.g., Chiodini *et al* 1998, Cardellini 2003a, 2003b, Frondini *et al* 2004, Nolasco *et al* 2008, Raco *et al* 2010). The total LFG output and the relative 95% confidence interval is then estimated through the AMRD and Sichel's estimator (table 3). For the statistical distribution of raw data, each survey shows different peculiarities for both of the analysed gases, about the number and numerosity of distinguished statistical populations. It is quite common to observe significant differences in the quantile–quantile plot of CO_2 and CO_4, anyway; usually the two components show a very similar pattern to the one displayed in figure 4, with a

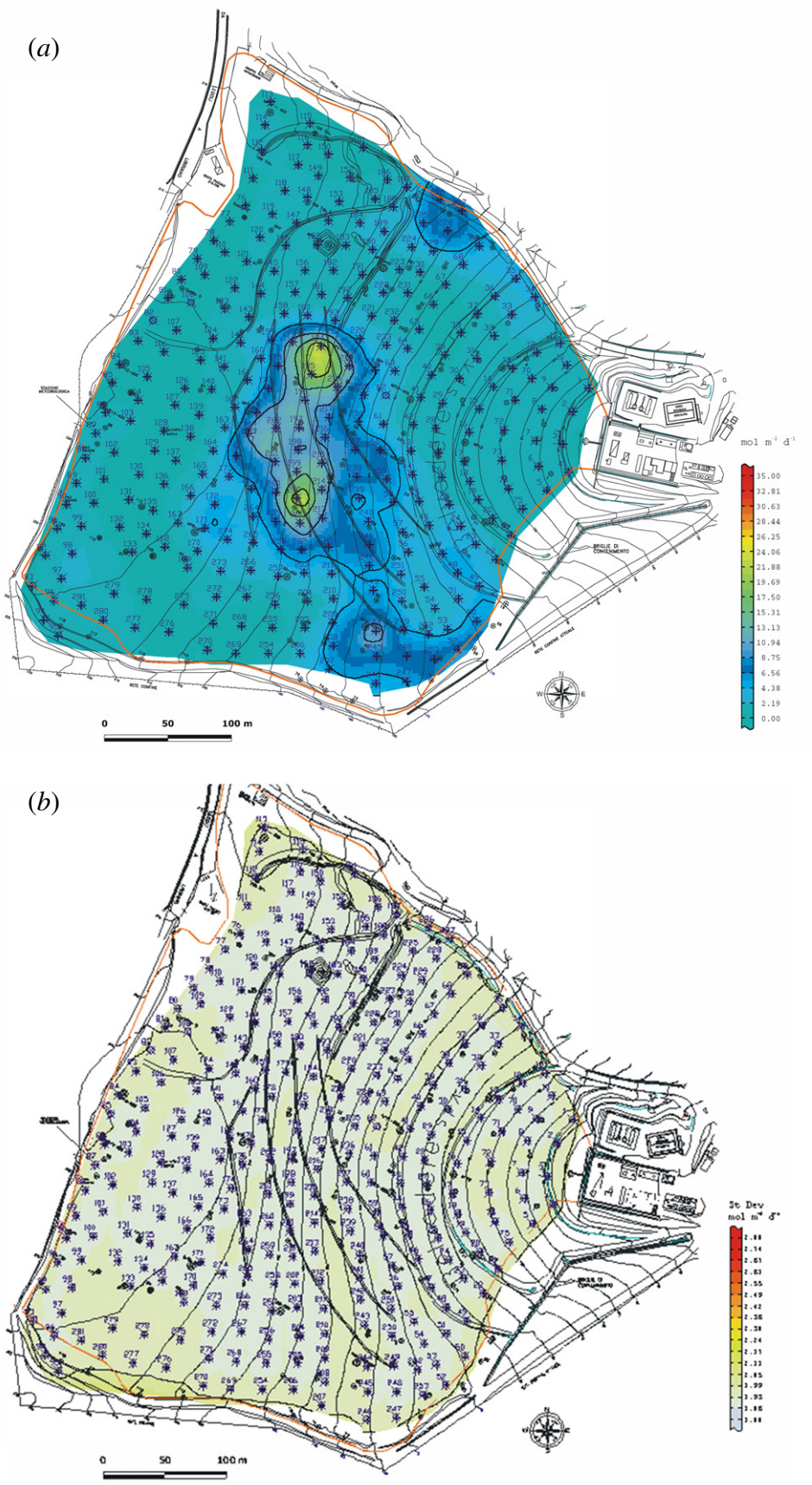

Figure 3. Isoflux map (*a*), standard deviation map (*b*), variogram (*c*) and mathematical model (*d*) relating to the June 2010 survey.

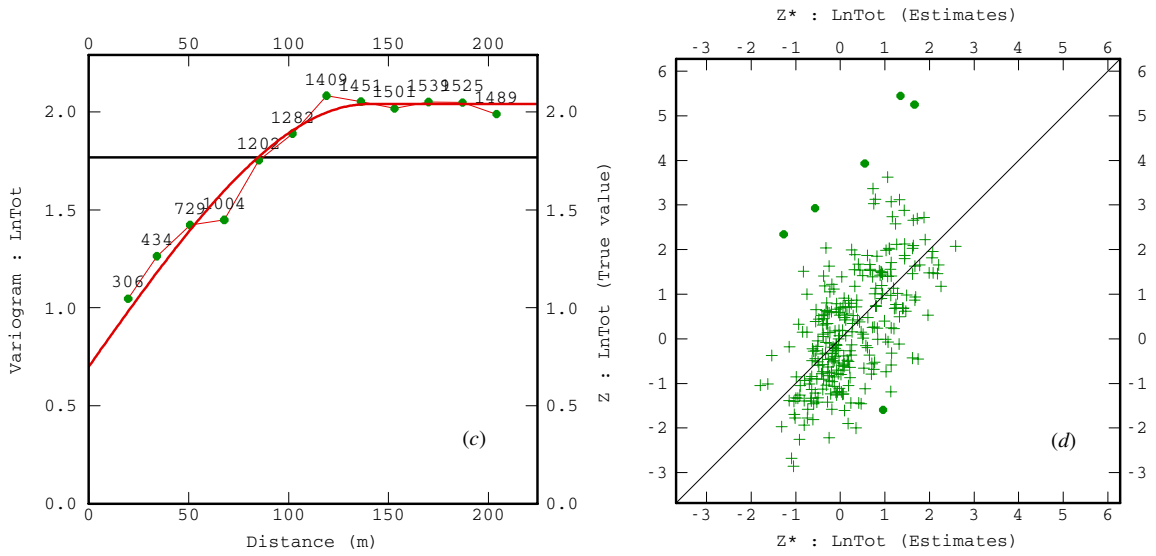

Figure 3. (continued)

Table 2. The main geostatistical parameters. The double parameters shown for December 2010 are due to the combination of models needed to achieve the best fit to the experimental variogram.

Survey	Range (m)	Sill	Nugget sill
May 2004	148	0.2	1.2
October 2004	84	2.1	–
January 2005	105	0.8	0.5
May 2005	116	0.8	1.4
October 2005	124	0.6	1
May 2006	79	0.8	1.4
October 2006	96	0.6	1.2
June 2007	123	0.6	1
November 2007	80	1.4	1.8
July 2008	90	0.8	1.5
January 2009	135	1.6	2.1
June 2009	140	1.14	1.85
December 2009	175	2.35	1
June 2010	140	1.34	0.7
December 2010	140	1.2	1
	80	0.6	
May 2011 (exponential model)	63	1.22	0.74
November 2011	97	2.48	2.13
May 2012	50	0.79	0.67
November 2012	47	1	1.02

number of recognizable statistical populations varying from 1 to a maximum of 4.

Taking into account the nineteen flux surveys (table 3), the total LFG output (CO_2 + CH_4) ranges from 111 to 1223 mol min^{-1}, and the total CO_2 and CH_4 outputs vary from 72 to 685 mol min^{-1} and from 33 to 618 mol min^{-1}, respectively, with average values of 283 and 178 mol min^{-1}. When the system is at rest, like in October 2004, the specific LFG flux (SF in table 3) is 15.7 mol m^{-2} d^{-1}, whereas when the collecting system is operating, the total specific flux ranges from 1.3 to 11.5 mol $m^{-2}d^{-1}$, with an average value of 5.06 mol m^{-2} d^{-1} and the CH_4 specific flux varies from 0.38 to 3.95 mol m^{-2} d^{-1}.

Figure 5 shows an increasing trend of total output of CO_2 and CH_4 diffuse from landfill cover from 2004 to 2006 (excluding October 2006 when the collecting system was at rest) and a meaningful decrease between October 2006 and May 2007, while the MSW disposal was still in activity and an increase in the LFG diffused from the cover was expected. Actually, this sharp decrease of LFG emission derives from remedial works driven by the indications obtained from previous gas flux surveys.

On December 2007 the collection of wastes was stopped. This is reflected by gas emission in a decreasing trend from July 2008 to December 2010, with only one exception in June 2009. This anomalous value is due to a partial and temporary stop of the collecting system. From December 2010 up to now the specific flux fluctuates in the range 1.3 to 2.3 mol m^{-2} d^{-1}.

As described above, the evaluation of the collecting system efficiency needs the evaluation of POG. In figure 6, CO_2-POG and CH_4-POG are shown with the output of a numerical production model (IPCC) and the calculated efficiency of the system.

The IPCC model underestimates LFG production up to October 2006. In later periods, the numerical model seems to fit the total estimated LFG production quite well. The improvement of model reliability has been achieved by the continuous calibration of the model driven by the gas flux measurements.

From figure 6, the meaningful decrease in LFG emission between October 2006 and May 2007 seems to reflect a reduction in the total LFG production; in fact the drop down of POG does not correspond to an increment of collected LFG. This decrease could be due to a lack of available water for the anaerobic methanogenic processes described by Themelis and Ulloa (2006):

$$C_6H_{10}O_4 + 1.5\ H_2O_{(liq)} \leftrightarrow 3.25\ CH_4 + 1.75\ CO_2. \quad (11)$$

This reaction can efficiently take place only if a suitable amount of water is present in the system. It is possible that the new clayey cover placed onto the whole landfill surface caused a reduction in the water infiltration rate that mitigated

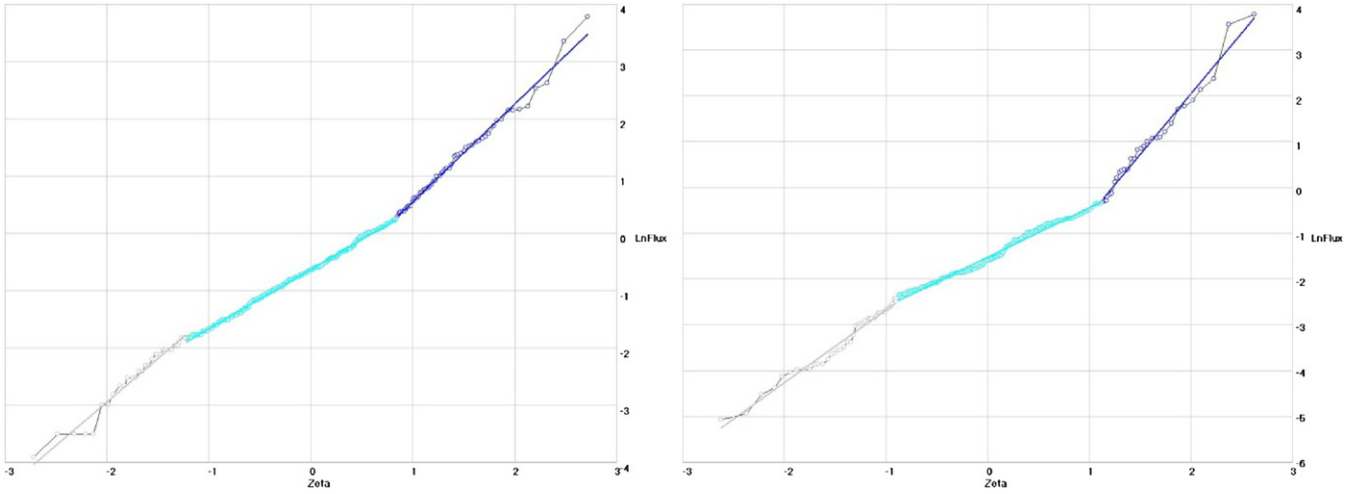

Figure 4. Q–Q plot relative to log-transformed flux data (May 2012) of CO_2 (left) and CH_4 (right).

Table 3. Total estimation results. Data are expressed in mol min^{-1}.

Survey	Surface m^2	Gas	Points	Output	95% Conf. Int. Upp. Limit	95% Conf. Int. Low. Limit	SF mol $d^{-1}m^{-2}$	POG	CH_4 ox %	Capt	EFF %
May 2004	64 000	CO_2 Tot	100	157	205	129	3.65	144 ± 2		411	56
		CH_4 Tot	42	142	245	101	3.30	167 ± 4	14.9 ± 2.0		
October 2004	112 000	CO_2 Tot	161	605	825	481	8.04	576 ± 4		0	0
		CH_4 Tot	166	618	802	525	8.21	676 ± 9	8.6 ± 1.2		
January 2005	118 000	CO_2 Tot	89	234	281	203	2.95	216 ± 3		593	32
		CH_4 Tot	113	216	273	183	2.73	251 ± 5	13.7 ± 1.9		
May 2005	128 000	CO_2 Tot	192	423	568	335	4.92	343 ± 13			40
		CH_4 Tot	189	212	306	163	2.47	372 ± 25	42.7 ± 3.9		
Oct 2005	120 000	CO_2 Tot	188	437	526	379	5.42	345 ± 15			52
		CH_4 Tot	158	182	271	142	2.26	367 ± 29	50.1 ± 4.0		
May 2006	107 500	CO_2 Tot	158	506	649	416	7.01	411 ± 15		533	42
		CH_4 Tot	152	256	320	219	3.54	446 ± 30	42.4 ± 3.9		
October 2006	130 000	CO_2 Tot	210	685	827	588	7.84	559 ± 20			43
		CH_4 Tot	159	356	457	292	4.07	608 ± 39	41.1 ± 3.8		
May 2007	116 000	CO_2 Tot	227	278	324	245	3.57	230 ± 7		564	46
		CH_4 Tot	148	156	192	134	2.00	252 ± 15	38.0 ± 3.7		
November 2007	116 500	CO_2 Tot	234	303	362	265	3.87	256 ± 7			47
		CH_4 Tot	148	190	248	156	2.43	284 ± 15	32.7 ± 3.5		
July 2008	130 500	CO_2 Tot	342	323	362	294	3.68	276 ± 7		500	42
		CH_4 Tot	204	216	278	176	2.46	308 ± 15	29.9 ± 3.3		
January 2009	130 500	CO_2 Tot	269	217	287	177	2.47	191 ± 4		521	40
		CH_4 Tot	180	165	229	133	1.88	217 ± 8	23.7 ± 2.9		
June 2009	128 500	CO_2 Tot	301	310	358	277	3.59	265 ± 7		410	42
		CH_4 Tot	219	204	247	178	2.37	295 ± 4	30.5 ± 3.4		
December 2009	125 000	CO_2 Tot	269	180	215	155	2.14	159 ± 3		405	54
		CH_4 Tot	164	140	180	115	1.67	181 ± 6	22.4 ± 2.8		
June 2010	122 500	CO_2 Tot	278	168	217	137	2.04	132 ± 6		410	60
		CH_4 Tot	174	70	88	58	0.84	141 ± 11	50.2 ± 4.0		
December 2010	122 500	CO_2 Tot	188	72	87	61	0.87	59 ± 2		350	74
		CH_4 Tot	103	39	64	29	0.47	64 ± 4	39.1 ± 3.8		
May 2011	125 000	CO_2 Tot	360	90	123	71	1.07	69 ± 3		410	74
		CH_4 Tot	275	33	46	27	0.39	73 ± 5	54.6 ± 3.9		
November 2011	132 000	CO_2 Tot	264	178	276	136	2.01	130 ± 8		300	53
		CH_4 Tot	180	36	48	29	0.40	132 ± 15	72.5 ± 3.2		
May 2012	143 000	CO_2 Tot	298	108	125	96	1.12	84 ± 4		335	63
		CH_4 Tot	225	41	55	34	0.42	89 ± 8	53.6 ± 4.0		
November 2012	143 000	CO_2 Tot	222	115	188	88	1.20	106 ± 1		457	67
		CH_4 Tot	190	106	204	75	1.10	123 ± 3	14.0 ± 1.9		

the methanogenesis process. Irrespective of considerations concerning both reactions (8) and the stoichiometry of the organic matter involved in it, it is known that water can play a significant role from the kinetic point of view, enhancing the rate of the disproportionation of organic matter (De Visscher and Van Cleemput 2003).

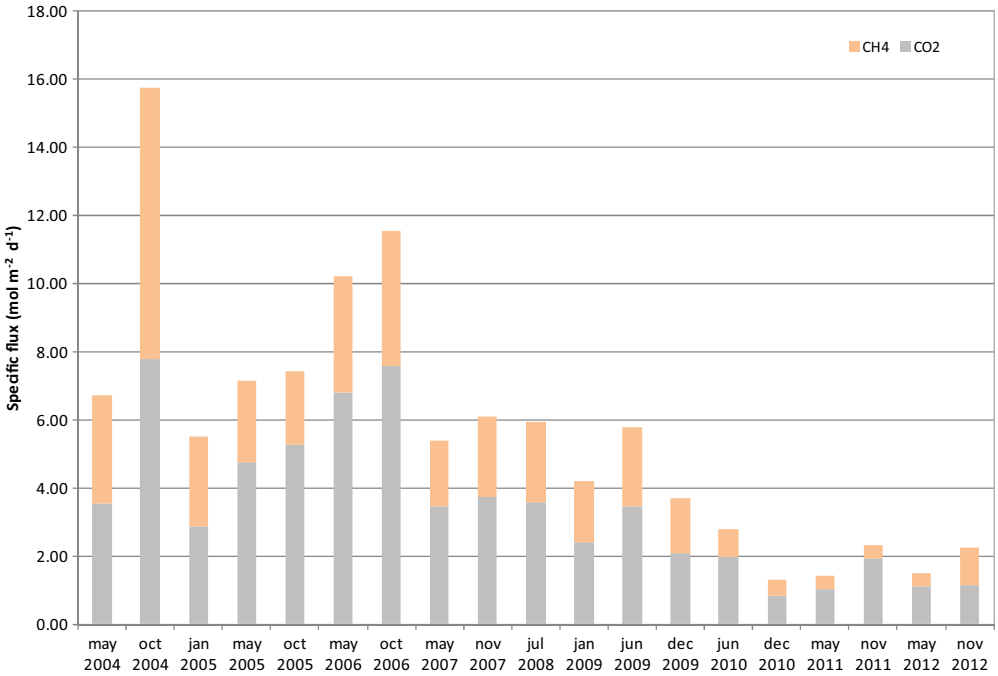

Figure 5. The specific flux of CO_2 and CH_4 emitted from the landfill cover.

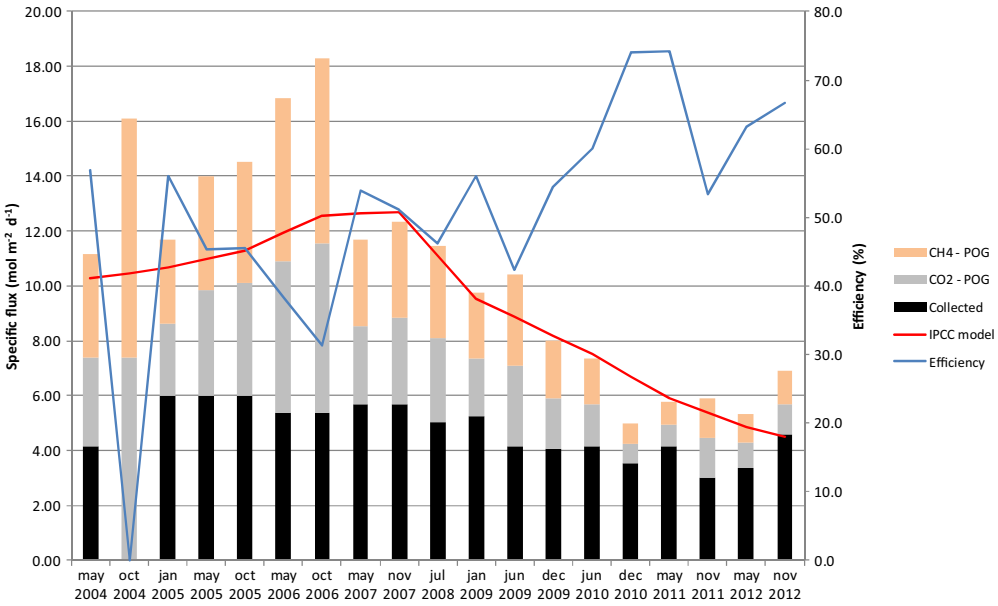

Figure 6. Comparison among IPCC numerical production models (red line), results obtained with direct measurements of flux (CH_4-POG, pre-oxidation CH_4; CO_2-POG, pre-oxidation CO_2), collected LFG (black bars) and recovery system efficiency (blue line).

In figure 6, the efficiency of the collecting system is also reported. These values, obtained using POG estimation, range from 31 to 74% with a general increasing trend.

Infrared thermography

Figure 7(*b*) shows the result of the thermographic survey made in the same period of the biogas flux measurements. A preliminary understanding of the observed thermal patterns is facilitated by the picture taken in the visible band from the same view point (figure 7(*a*)). The scene mapped by infrared radiometry has a good overall coherence with the mapped fluxes of biogas release (figure 3(*a*)), and proves how the combination of the two different techniques is informative, by providing additional elements for a proper interpretation.

In this particular case, a recently disturbed landfill cover (dashed area in figure 7(*b*)) exhibits a thermal anomaly that is not associated with flux anomalies, as expected. An interesting correspondence between patterns in the thermal map and in the map of fluxes is easily identified by taking the letters of the label 'Belvedere SpA' as a reference. In this context, the most significant relative thermal anomalies are pointed out by black arrows, and are located similarly to the areas of higher

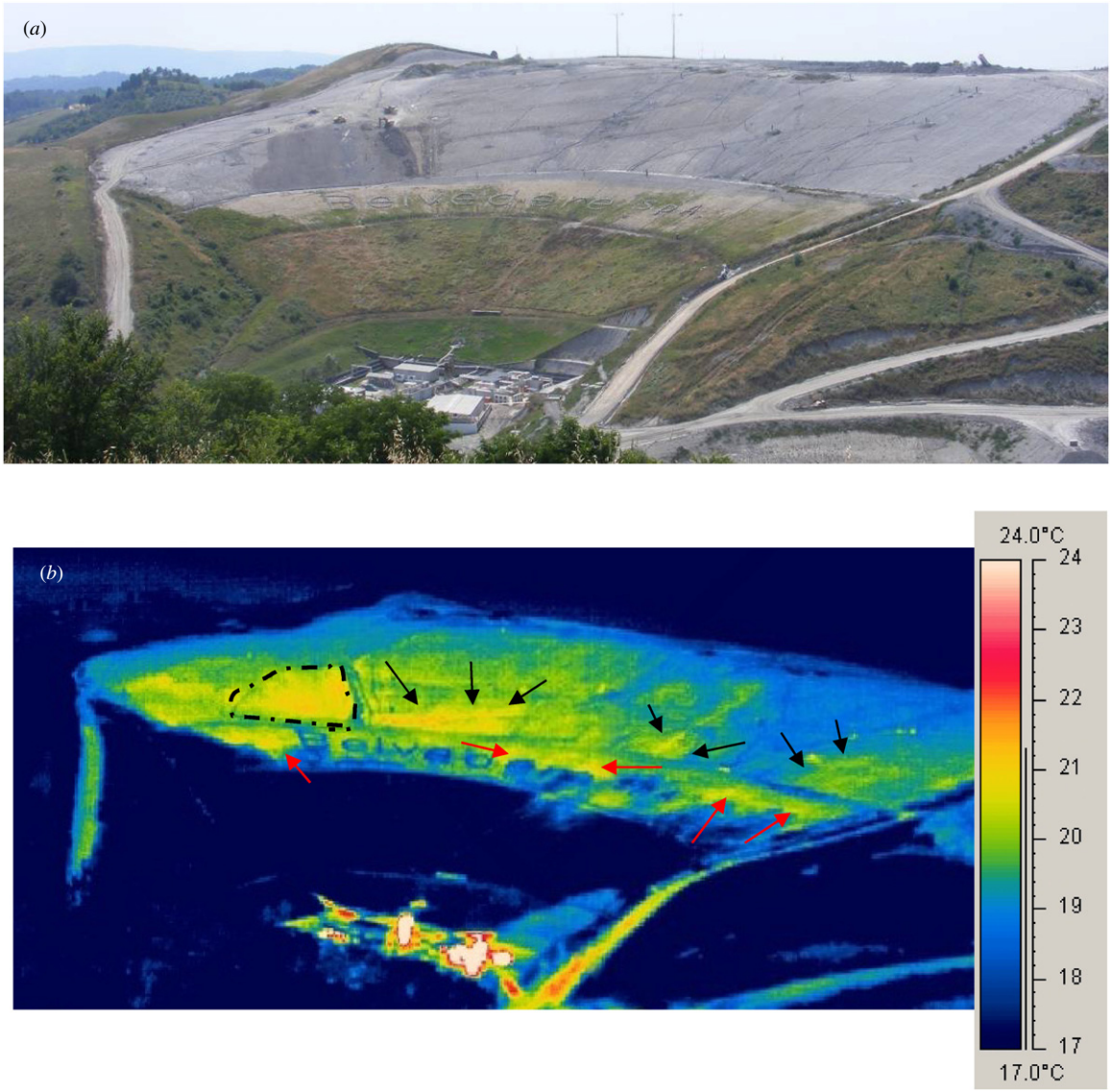

Figure 7. Front view of the investigated site (pictures taken in June 2010). Visible band (*a*) and thermal map (*b*) obtained by long-wave infrared radiometry.

fluxes shown in figure 3(*a*), i.e., just above the vegetated area. Instead, red arrows indicate relative thermal anomalies that are not reflected by the map of fluxes, presumably due to the different nature of the vegetated layer with respect to the upper part of the landfill, which has still the clay coverage. In particular, peculiarities of the observed surfaces, such as the kind of material, its shape, its humidity and the degree of contact with the surrounding soil, contribute to determining its variable radiometric properties, justifying the variable apparent temperatures of the observed bodies. This particular aspect shows how the infrared radiation thermometry is a non-trivial issue, and enforces the need to combine different techniques, in order to get more elements for the interpretation and validation of results, by cross-checking the information.

As stated before, environmental applications do not usually allow easily repeatable absolute temperature assessments made by radiation termometry, mainly due to the variability of the environmental and target conditions. It is instead reasonable to make good use of such quantitative assessments by using some interpretation technique like the usage of reference targets. Thus, a direct comparison of absolute values between different campaigns is unlikely to be meaningful as a general idea, while the interpretation of the development of the monitored system, by an appropriate interpretation of the observable patterns and their evolution in time, can open the way to strong monitoring possibilities.

Figures 8 and 9 show an example of the evolution of the investigated site in the successive two years (2011 and 2012) with respect to figure 7. In order to get a similar false colour distribution in the two pictures, different colour scales have been assigned, as a further proof of the said variability that characterizes this kind of scenario. Under the hypothesis that vegetation is an opaque target with constant emissivity, which assumes the same temperature of its surrounding air, it is apparent how the 2012 (figure 9) campaign was performed at a lower atmospheric temperature than the 2011 one (figure 8). Thus, after proper colour scale assignment, some common

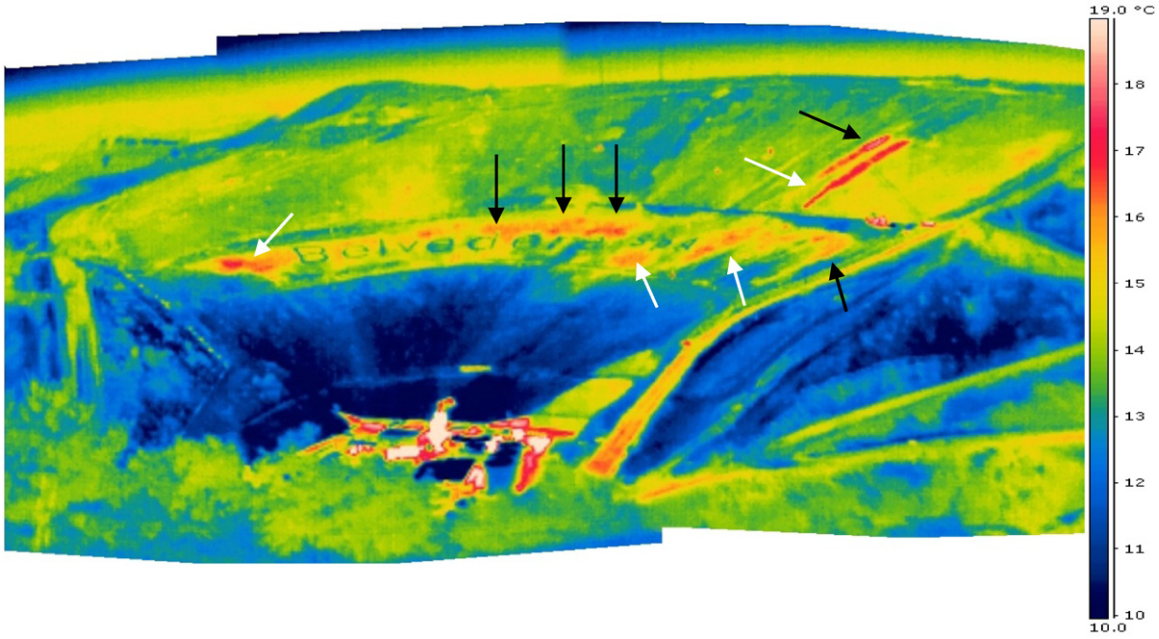

Figure 8. Front view of the investigated site (picture taken in May 2011). Thermal map obtained by long-wave infrared radiometry.

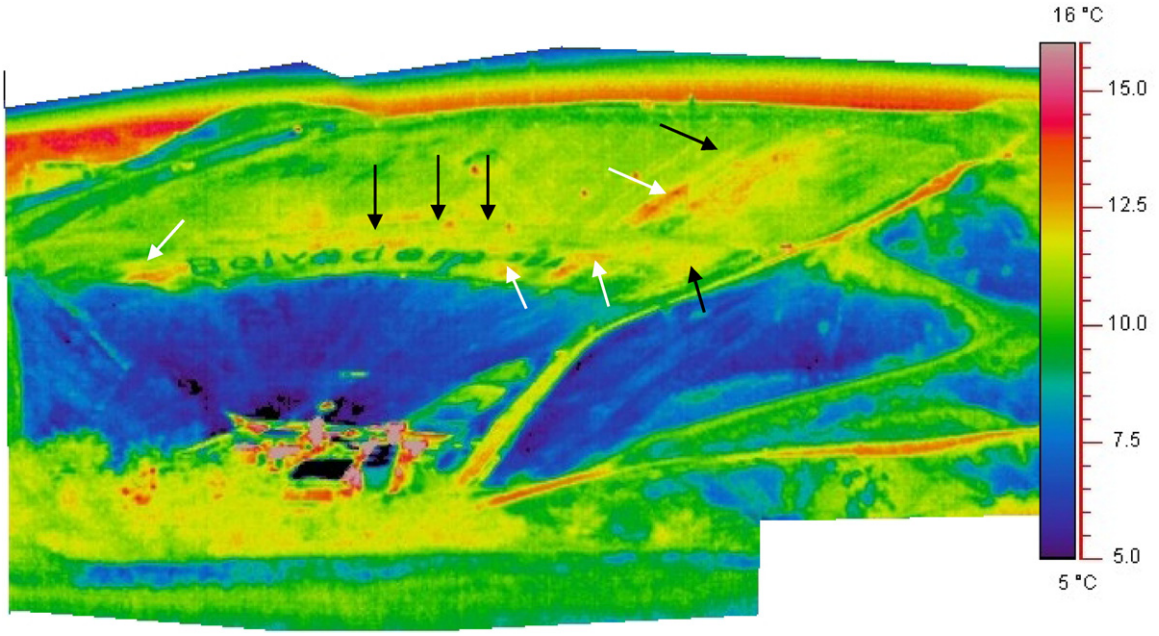

Figure 9. Front view of the investigated site (picture taken in May 2012). Thermal map obtained by long-wave infrared radiometry.

patterns between figures 8 and 9 can still be identified and commented upon. White arrows indicate patterns that can be individuated in both campaigns, with some degree of attenuation in the more-recent campaign. They are mostly areas characterized by recently moved and compacted clay, partly observable also in the 2010 campaign. It is important to note that some patterns have substantially disappeared in the latest campaign (e.g., those noted by black arrows), while a particular activity of the gas collecting system in the 2012 campaign is appreciable by observing the biogas wells in figure 9, which are clearly detectable as positive thermal anomalies.

Conclusions

The estimation of the total LFG output carried out by the methodology adopted in this study, which is based on the measurement of the real amounts of CH_4 and CO_2 discharged into the atmosphere, is a reliable and useful tool for landfill management, from both the environmental and the economic points of view. The adopted method is based on punctual measurements of CO_2 and CH_4 flux carried out by means of the accumulation chamber technique. The data processing consists in the partitioning of the statistical population and the subsequent evaluation of AMRD for each recognized subset.

This procedure allows us to evaluate the total LFG output (within a 95% confidence interval) released to the atmosphere. Moreover, isoflux maps, drawn by using the lognormal kriging methodology, allow an easy and clear visualization of the areas characterized by high LFG fluxes. This crucial information permits us to define proper remedial works in order to improve the effectiveness of the landfill cover and the efficiency of the collecting system.

Thermographic images have been taken with a long-wave IR radiometer in for each survey; this additional monitoring technique enhances the possibility of understanding the observed processes, by individuating the degree of correlation between relative thermal anomalies and the biogas fluxes mapped. As discussed in this paper, relative thermal anomalies do not necessarily resemble anomalous flux releases, but the complex relationship between the two investigation methods carries additional fruitful information about the studied site.

These kinds of measurements are also a fundamental step in properly setting up an LFG numerical production model that, with an effective calibration on measured data, can become an useful tool to forecast the residual potentiality of the plant.

It is worth mentioning that these kind of studies, if carried out on a large scale, may bring a significant global increase in the recovered energy from landfill sites, by reducing the contribution to the total anthropogenic methane originating from the disposal of waste.

Acknowledgments

Many thanks go to Belvedere SpA (the company which manages the Legoli landfill) for their constant availability and receptive attitude. Finally, the availability of these data is due to West Systems Srl, who are the manufacturer of the automatic monitoring devices for biogas flux measurement.

References

Anthony C 1982 *Methanogens and methanogenesis The Biochemistry of Methylotrophs* (London: Academic) pp 296–327

Armstrong M 1984a Problems with universal kriging *Math. Geol.* **16** 101–8

Armstrong M 1984b Problems with universal kriging *Math. Geol.* **16** 305–16

Balch W E, Woese C R and Wolfe R S 1979 Methanogens: re-evaluation of a unique biological group *Microbiol. Rev.* 260–96

Barlaz M A, Ham R K and Schafer D M 1989 Mass balance analysis of decomposed refuse in laboratory scale lysimeters *J. Environ. Eng.* **115** 1088–102

Boone D R and Bryant M P 1980 Propionate–degrading bacterium, *Syntrophobacter wolinii*, from methanogenic ecosystems *Appl. Environ. Microbiol.* **40** 626–32

Cardellini C, Chiodini G and Frondini F 2003a Application of stochastic simulation to CO_2 flux from soil: mapping and quantification of gas release *J. Geophys. Res.* **108** 2165

Cardellini C, Chiodini G, Frondini F, Granieri D, Lewicki J and Peruzzi L 2003b Accumulation chamber measurements of methane fluxes: application to volcanic-geothermal areas and landfills *Appl. Geochem.* **18** 45–54

Chanton J and Liptay K 2000 Seasonal variation in methane oxidation in a landfill cover soil as determined by an *in situ* stable isotope technique *Glob. Biogeochem. Cycles* **14** 51–60

Chauvet P 1982 The variogram cloud Proceedings of the 17th APCOM Symposium ed T B Johnson and R J Barnes (New York: Society of Mining Engineers) pp 757–64

Chauvet P 1991 *Aide mémoire de géostatique linéeaire-Chaiers de géostatistique, Fascicule 2* (Fontainebleau: Ecole des Mines de Paris) p 210

Chauvet P 1993 *Processing Data with a Spatial Support: Geostatistics and its Method-chaiers de géostatique, Fascicule n. 4* (Fontainebleau: Ecole des Mines de Paris) p 57

Chauvet P and Galli A 1982 *Universal Kriging* (Fontainebleau: Ecole des Mines de Paris) (Publication no. C-96)

Chiodini G, Cioni R, Guidi M, Marini L and Raco B 1998 Soil CO_2 flux measurements in volcanic and geothermal areas *Appl. Geochem.* **13** 543–52

Chiodini G, Frondini F and Raco B 1996 Diffuse emission of CO_2 from the fossa crater, vulcano island (Italy) *Bull. Volcanol.* **58** 41–50

Clark I 1979 *Practical Geostatistics* (London: Department of Mineral Resources Engineering, Royal School of Mines, Imperial College of Science and Technology) p 129

Czepiel P, Mosher B, Crill P and Harriss R 1996 Quantifying the effect of oxidation on landfill methane emissions *J. Geophys. Res.* **101** 16721–9

David M 1977 *Geostatistical ore Reserve Estimation* (Amsterdam: Elsevier)

Davis J 1986 *Statistics and Data Analysis in Geology* 2nd edn (New York: Wiley) p 646

De Visscher A and Van Cleemput O 2003 Simulation model for gas diffusion and methane oxidation in landfill cover soils *Waste Manag.* **23** 581–91

DeWitt D P and Nutter G D 1988 *Theory and Practice of Radiation Thermometry* 1st edn (New York: Wiley-Interscience) pp 1152

El-Fadel M, Findikakis A and Leckie J 1988 A numerical model for methane production in managed sanitary landfills *Waste Manag. Res.* **7** 31–42

Findikakis A and Leckie J 1979 Numerical simulation of gas flow in sanitary landfills *J. Environ. Eng. Div.* **105** 927–45

Findikakis A, Papelis C, Halvadakis C and Leckie J 1987 Modelling gas production in managed sanitary landfills *Waste Manage. Res.* **6** 115–23

Frondini F, Chiodini G, Caliro S, Cardellini C, Granieri D and Ventura G 2004 Diffuse CO_2 degassing at vesuvio, Italy *Bull. Volcanol.* **66** 642–51

Gaussorgues G 1993 *Infrared Thermography (5th edition of Microwave Technology Series)* 5th edn (Berlin: Springer) p 508

Hashemi M, Kavak H I, Tsotsis T T and Sahimi M 2002 Computer simulation of gas generation and transport in landfills: I. Quasi-steady-state condition *Chem. Eng. Sci.* **57** 2475–501

Hinkle M 1994 Environmental conditions affecting concentrations of He, CO_2, O2 and N2 in soil gases *Appl. Geochem.* **9** 53–63

Hinkle M and Ryder J L 1987 Meteorological variables and concentrations of helium, carbon dioxide, and oxygen in soil gases collected regularly at a single site for more than a year *U.S. Geological Survey Open-File Report* 87-449

Hinkle M and Ryder J L 1988 Effect of meteorological changes on concentration of helium, carbon dioxide and oxygen, in soil gases *SME Ann. Meeting (Phoenix, AZ)*

Journel A and Huijbregts C 1978 *Mining Geostatistics* (London: Academic Press) p 600

Kanemasu E, Power W and Sij J 1974 Field chamber measurements of CO_2 flux from soil surface *Soil Sci.* **118** 233–7

King C and Minissale A 1994 Seasonal variability of soil gas radon concentration in central California *Radiat. Meas.* **23** 683–92

Kirshop B H 1984 Methanogenesis *CRC Crit. Rev. Biotech.* **1** 109–59

Kising A and Socolow R 1994 Human impact on the nitrogen cycle *Phys. Today* **47** 24–31

Krige D 1951 A statistical approach to some basic mine valuation problems on the witwatersrand *J. Chem. Metall. Min. Soc. South Afr.* **52** 119–39

Kucera C and Kirkham D R 1971 Soil respiration studies in tall grass prairie in Missouri *Ecology* **52** 912–5
Le Mer J and Roger P 2001 Production, oxidation, emission and consumption of methane by soils: a review *Eur. J. Soil Biol.* **37** 25–50
Li H, Sanchez R, Joe Qin S, Kavak H I, Webster I A, Tsotsis T T and Sahimi M 2011 Computer simulation of gas generation and transport in landfills: V. Use of artificial neural network and the genetic algorithm for short- and long-term forecasting and planning *Chem. Eng. Sci.* **66** 2646–59
Mah R A and Smith M R 1981 The methanogenic bacteria *The Prokaryotes: a Handbook on Habitats, Isolation and Identification of Bacteria* vol 1 (New York: Springer) pp 948–77
Manna L, Zanetti M and Genon G 1999 Modelling biogas production at landfill site *Resources Conserv. Recycling* **26** 1–14
Martini I and Sagri M 1993 Tectonosedimentary characteristic of late miocene-quaternary extensional basins of the Northern Appennines *Earth Sci. Rev.* **34** 197–233
Matheron G 1962 *Traité de Géostatique Appliqué* (Paris: Technip)
Matheron G 1965 *Les variables Regionalisées et leur estimation* (Paris)
Matheron G 1969 *Le Krigeage universel, Fascicule n. 1* (Fontainebleau: Les Cahiers du Centre De Morphologie Mathématique. Ecole des Mines de Paris)
Matheron G 1970 *The Theory of Regionalized Variables and its Applications, Fascicule n. 5* (Paris: Techinip)
Mazzanti R 1961 Geologia della zona di montaione tra le valli dell'Era e dell'Elsa (Toscana) *Boll. Soc. Geol. It.* **80** 37–126
McInerey M J and Bryant M P 1980 Syntrophic associations of H2 utilizing methanogenic bacteria and H2 producing alcool and fatty acid—degrading bacteria in anaerobic degradation of organic matter *Anaerobes and Anaerobic Infections* (New York: Gustav Fisher) pp 117–26
McInerey M J and Bryant M P 1981a Basic principles of bioconversions in anaerobic digestion and methanogenesis *Biomass Conversion Processes for Energy and Fuels* (New York: Plenum) pp 277–96
McInerey M J and Bryant M P 1981b Review of methane fermentation fundamentals *Fuels and Gas Production from Biomass* (West Palm Beach, FL: Chemical Rubber) pp 19–46
Nastev M, Therien R, Lefebvre R and Gélinas P 2001 Gas production and migration in landfills and geological materials *J. Contam. Hydrol.* **52** 187–211
Nolasco D, Lima N L, Hernández P A and Pérez N M 2008 Non-controlled biogenic emissions to the atmosphere from lazare to landfill, Tenerife, Canary Islands *Environ. Sci. Pollut. Res.* **15** 51–60
Parkinson K 1981 An improved method for measuring soil respiration in the field *J. Appl. Ecol.* **18** 221–8
Pinoult J and Baubron J 1996 Signal processing of soil gas radon, atmospheric pressure, moisture, and soil temperature data: a new approach for radon concentration modelling *J. Geophys. Res.* **101** 3157–71
Raco B, Battaglini R and Lelli M 2010 Gas emission into the atmosphere from controlled landfills: an example from legoli landfill (Tuscany, Italy) *Environ. Sci. Pollut. Res.* **17** 1197–206
Raco B, Scozzari A, Guidi M, Lelli M and Lippo G 2005 Comparison of two non-invasive methodologies to monitor diffuse biogas emissions from MSW landfills soil: a case study *Proc. Sardinia 2005, 10th Int. Waste Manag. and Landfill Symp. (Cagliari, Italy)*
Reimer G M 1980 Use of soil gas helium concentration for earthquake prediction: limitation imposed diurnal variation *J. Geophys. Res.* B **85** 3107–14
Scharff J 2006 Applying guidance for methane emission estimation for landfills *Waste Manag.* **26** 417–29
Scozzari A 2008 Non-invasive methods applied to the case of municipal solid waste landfills (MSW): analysis of long-term data *Adv. Geosci.* **19** 33–38
Sichel H 1966 The estimation of means and associated confidence limits for small samples for lognormal population *Symp. on Mathematical Statistics and Computer Applications in Ore Valuation (South African Institute of Mining and Metallurgy, Johannesburg)* pp 106–23
Simpson V and Anastasi C 1993 Future emissions of CH_4 from the natural gas and coal industries *Energy Policy* **21** 827–30
Sinclair A 1974 Selection of threshold values in geochemical data using probability graphs *J. Geochem. Explor.* **3** 129–49
Sinclair A 1991 A fundamental approach to threshold estimation in exploration geochemistry: probability plots revisited *J. Geochem. Explor.* **41** 1–22
Singh A 1993 Omnibus robust procedures for assessment of multivariate normality and detection of multivariate outliers *Multivariate Environmental Statistics* ed G Patil and C Rao (Amsterdam: Elsevier) pp 445–88
Singh A, Singh A K and Engelhardt M 1997 The lognormal distribution in environmental applications *Technology Support Center Issue,* EPA/600/S-97/006
Themelis N and Ulloa P 2006 Methane generation in landfills *Renew. Energy* **32** 1243–57
Tonani F and Miele G 1991 Methods for measuring flow of carbon dioxide through soils in volcanic setting *Int. Conf. on Active Volcanoes and Risk Mitigation (Napoli)*
Trégourès A, Beneito A, Berne P G, Sabroux J C, Savanne D, Pokryszka Z and Burkhalter R 1999 Comparison of seven methods for measuring methane flux at a municipal solid waste landfill site *Waste Manag. Res.* **17** 453–8
Virgili G, Continanza D and Coppo L 2008 The FLUX-meter: a portable integrated instrumentation for the measurement of the biogas diffuse degassing from landfills *G. Geologia Appl.* **9** 73–84
Wackernagel H 1995 *Multivariate Geostatistics* (Berlin: Springer)
Whitman W B 1985 *Methanogenic bacteria Archaebacteria* (New York: Academic Press) pp 3–84
Witkamp M 1969 Cycles of temperature and carbon dioxide evolution from litter and soil *Ecology* **50** 922–4
Wolfe R S 1971 Microbial formation of methane *Adv. Microb. Physiol.* **6** 107–46
Zeikus J G 1977 The biology of methanogenic bacteria *Bacteriol. Rev.* **41** 514–41